



A DFT study on the mechanical properties of Co_9S_8 during the lithiation/sodiation process

YANHUI DING^{1,*} , WENWU JIANG^{1,2} and XIANQIONG TANG¹

¹Institute of Rheological Mechanics, Xiangtan University, Xiangtan 411105, China

²School of Civil Engineering, Wuhan University, Wuhan 430072, China

*Author for correspondence (yhding@xtu.edu.cn)

MS received 20 May 2022; accepted 19 August 2022

Abstract. Cobalt sulphides, including CoS , CoS_2 , Co_3S_4 and Co_9S_8 , have been studied as potential anode materials for Li- and Na-ion batteries. However, the mechanical properties of the cobalt sulphides have not been intensively investigated. In this work, density functional theory (DFT) calculation was employed to study the mechanical properties of the cobalt sulphides mentioned above. Besides, the mechanical properties of final products of lithiation/sodiation of Co_9S_8 have been calculated, including the bulk modulus, shear modulus, Young's modulus and Poisson's ratio. This work provides an insight into understanding the electrochemical performance of Co_9S_8 material as anode material for Li- and Na-storage during the cycling process.

Keywords. Cobalt sulphides; DFT; mechanical properties; lithiation process; modulus.

1. Introduction

Development of new materials for Li-ion batteries (LIBs) has received a great deal of attention in recent years due to the disadvantages of the existing electrode materials [1–3]. In the case of anode materials, graphite has been widely used in commercial LIBs. However, the low theoretical capacity of graphite does not meet the consumer's need for batteries with high energy density [4]. Thus, extensive efforts have been devoted to exploring new anode materials with a high capacity for advanced LIBs [5–8]. Recently, nanostructured carbon materials including graphene, nanotubes, nanofibres and porous carbon have been intensively investigated [9–12]. The capacity of these carbonous materials is higher than the theoretical capacity of graphite. The drawbacks of these carbonous anodes include the low charging/discharging efficiency at the first cycle and the poor dispersion stability.

Transition metal sulphides have been considered as promising candidates for graphite anode materials due to their high theoretical capacity [13,14]. However, the application of transition metal sulphides is greatly prohibited by the large volume change during the lithiation process. Many strategies have been carried out to enhance the structural stability of transition metal sulphides, such as morphology modulation, surface coating and combination with carbon nanomaterials. In the family of transition metal sulphides, cobalt sulphides including the forms of CoS , CoS_2 , Co_3S_4 , and Co_9S_8 have been considered as potential

anode materials for LIBs and sodium-ion batteries owing to their high theoretical capacities and high electrical conductivity [15,16]. However, practical application of cobalt sulphides is limited by severe volume changes during the lithiation process and poor electrochemical kinetics, which causes poor cyclic stability and unsatisfactory rate capability. Several methods have been adopted to improve the electrochemical performance of cobalt sulphides, such as hybridization of cobalt sulphides with carbonaceous materials and construction of hierarchical structures. Although cobalt sulphides have been intensively studied, the structural evolution during the lithiation/sodiation process is still unrevealed from the view of mechanics. The rate capability and cycling performance of the electrode materials greatly depend on the structural stability. The Li insertion caused the lattice distortion of the electrode materials, and further resulted in the changes in bond length and angles. Usually, the bulk modulus is used to characterize a materials resistance to volume deformation against external pressure, while the shear modulus measures a materials ability to resist shear strain. That is, the mechanical properties of the materials often determine their structural stability and the applications.

Up to now, the mechanical properties of the cobalt sulphides have not been intensively investigated. Thus in this work, density functional theory (DFT) calculation was employed to study the mechanical properties of the cobalt sulphides mentioned above. Besides, the structural evolution of the most stable phase Co_9S_8 during the

lithiation/sodiation process has been calculated, including the bulk modulus, shear modulus, Young's modulus and Poisson's ratio.

2. Calculation method

Structural optimization and calculation of elastic constants of cobalt sulphides (CoS, CoS₂, Co₃S₄ and Co₉S₈) have been performed by CASTEP module built in Materials Studio, based on Perdew-Burke-Ernzerhof (PBE) theoretical framework. Electronic wavefunctions are expanded in a plane wave basis set with the kinetic energy cutoff of 600 eV. The *k*-points 13×13×8, 7×7×7, 7×7×7 and 4×4×4 were adopted for integration in the Brillouin zone. The convergence criterion of energy was set as 5.0×10⁻⁷ eV per atom. The maximum number of fully self-consistent field iteration steps is set to 300.

3. Results and discussion

The atomic structures of cobalt sulphides (hexagonal phase CoS, cubic phase CoS₂, cubic phase Co₃S₄ and cubic phase Co₉S₈) are presented in figure 1. The blue and yellow spheres indicate Co and S atoms, respectively. The crystal structures of the cobalt sulphides mentioned above have been investigated in literatures [17–20]. The space groups and lattice parameters of the cobalt sulphides are listed in table 1.

The calculated elastic constants of the cobalt sulphides mentioned above are listed in table 2. The values of elastic constants are all positive and satisfy the condition for mechanical stability. For hexagonal phase CoS, five elastic constants including C₁₁, C₁₂, C₁₃, C₃₃ and C₄₄ besides C₆₆

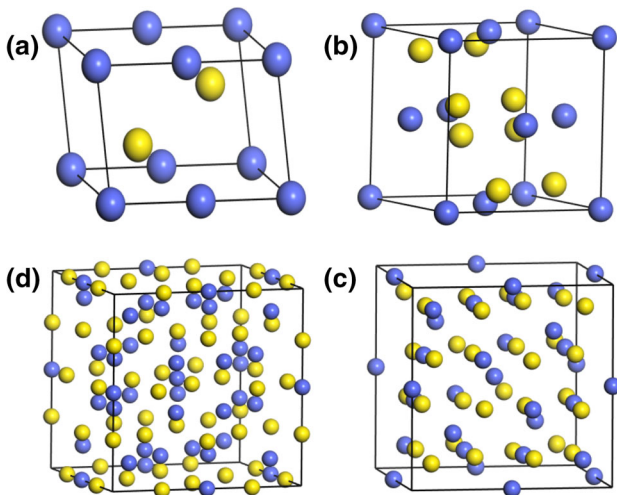


Figure 1. Atomic structures of cobalt sulphides: (a) hexagonal phase CoS; (b) cubic phase CoS₂; (c) cubic phase Co₃S₄; (d) cubic phase Co₉S₈.

Table 1. Structural parameters of cobalt sulphides.

Phase	Space group	Materials Id	<i>a</i> /Å	<i>b</i> /Å	<i>c</i> /Å
CoS	<i>P6₃/mmc</i>	mp-1183733	3.347	3.347	5.139
CoS ₂	<i>Pa $\bar{3}$</i>	mp-2070	5.506	5.506	5.506
Co ₃ S ₄	<i>Fd $\bar{3}m$</i>	mp-943	6.573	6.573	6.573
Co ₉ S ₈	<i>Fm $\bar{3}m$</i>	mp-1513	6.933	6.933	6.933

are independent, which can be employed to evaluate the stability status. The mechanical stability conditions, known as Born's criteria, can be found in the references [21]. The calculated elastic constants indicate that the CoS, CoS₂, Co₃S₄ and Co₉S₈ phases are theoretically stable. Due to the symmetry of the crystal structures, the C₁₁ = C₂₂ = C₃₃. For the cubic phase CoS₂, Co₃S₄ and Co₉S₈, C₁₂ = C₁₃ = C₂₃ and C₄₄ = C₅₅ = C₆₆.

The elastic constants can be further employed to calculate the mechanical properties of CoS, CoS₂, Co₃S₄ and Co₉S₈ phases. Two approximation methods, namely the Voigt's and Reuss's methods, have been widely used to calculate the bulk modulus (*K*) and shear modulus (*G*) [22].

For the cubic phase,

$$K_V = K_R = \frac{(C_{11} + 2C_{12})}{3}$$

$$G_V = \frac{1}{5}(C_{11} - C_{12} + 3C_{44})$$

$$G_R = \frac{5(C_{11} - C_{12})C_{44}}{3(C_{11} - C_{12}) + 4C_{44}} \quad (1)$$

For the hexagonal phase,

$$K_V = [2(C_{11} + C_{12}) + 4C_{13} + C_{33}]/9$$

$$K_R = [(C_{11} + C_{12})C_{33} - 2C_{13}^2]/(C_{11} + C_{12} + 2C_{33} - 4C_{13})$$

$$G_V = \frac{1}{30}(C_{11} + C_{12} + 2C_{33} - 4C_{13} + 12C_{44} + 12C_{66})$$

$$G_R = \frac{5C_{44}C_{66}[(C_{11} + C_{12})C_{33} - 2C_{13}^2]}{2[3K_V C_{44} C_{66} + \{(C_{11} + C_{12})C_{33} - 2C_{13}^2\}(C_{44} + C_{66})]} \quad (2)$$

The calculated results from Voigt's and Reuss's methods denote the upper and lower limits of the bulk modulus. Hill [23] proved that the arithmetic average value of Voigt's and Reuss's methods is closer to the real value.

$$K = \frac{1}{2}(K_V + K_R)$$

$$G = \frac{1}{2}(G_V + G_R) \quad (3)$$

Table 2. Elastic constants (C_{ij}) of CoS, CoS₂, Co₃S₄ and Co₉S₈.

Elastic constants (GPa)	CoS	CoS ₂	Co ₃ S ₄	Co ₉ S ₈
C_{11}	253.08660	221.83662	206.19952	268.93250
C_{22}	253.08660	221.83662	206.19952	268.93250
C_{33}	253.08660	221.83662	206.19952	268.93250
C_{12}	111.50940	62.79150	98.90419	120.20748
C_{13}	118.41484	62.79150	98.90419	120.20748
C_{23}	118.41484	62.79150	98.90419	120.20748
C_{44}	28.95405	74.95395	49.53421	68.15707
C_{55}	28.95405	74.95395	49.53421	68.15707
C_{66}	28.95405	74.95395	49.53421	68.15707

The Young’s modulus E and Poisson’s ratio ν can be calculated by the following relationship.

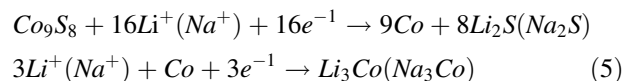
$$E = \frac{9KG}{3K + G}$$

$$\nu = \frac{3K - 2G}{2(3K + G)} \tag{4}$$

The bulk, shear, Young’s moduli and Poisson’s ratios of the four types of cobalt sulphides have been calculated as listed in table 3. Generally, the mechanical properties affect the electrochemical performance of the cathode materials. Besides the volume variation, Young’s modulus is also an important factor that determines the robustness of the cathode material during the charging/discharging process. Comparisons of the bulk, shear, Young’s moduli and Poisson’s ratios of the four types of cobalt sulphides are presented in figure 2. The cobalt sulphides exhibit different mechanical properties with the change of the stoichiometric ratio of Co/S. The high number of Li atoms incorporated into the cobalt sulphides during lithiation causes large volume changes. From the point of view of mechanics, the

insertion of Li atoms induces internal stress. High bulk modulus favours the Li insertion and extraction. From figure 2, it can be found that the CoS₂ phase shows the lowest value of bulk modulus (~115.81 GPa). As comparison, the Co₉S₈ phase exhibits a relatively high bulk modulus of 169.78 GPa. Thus, the Co₉S₈ phase with the highest value of bulk modulus shows great potential for application in anode materials.

Based on the discussion mentioned above, Co₉S₈ phase is worth further investigation among the four types of cobalt sulphides. The Co₉S₈ phase undergoes the electrochemical reaction in the lithiation/sodiation process and forms alloys as follows [11,24].



After full lithiation, a huge volume change ~450% was obtained. This is the reason for the capacity fading in the cycling. DFT calculation indicates that the Li₃Co (Na₃Co) phase is the most stable structure at the lowest energy state [11]. The atomic models of the Li₃Co and Na₃Co phases are shown in figure 3. As presented in figure 3a, the Li₃Co phase possesses a tetragonal crystal

Table 3. Moduli and Poisson’s ratios of the four types of cobalt sulphides.

Phase	Bulk modulus (GPa)	Shear modulus (GPa)	Young’s modulus E (GPa)	Poisson’s ratio ν
CoS	K_V 161.77	G_V 36.40	193.32	0.40
	K_R 161.74	G_R 32.62		
	K 161.76	G 34.51		
CoS ₂	K_V 115.81	G_V 76.78	188.59	0.23
	K_R 115.81	G_R 76.72		
	K 115.81	G 76.75		
Co ₃ S ₄	K_V 134.67	G_V 51.18	136.18	0.33
	K_R 134.67	G_R 51.10		
	K 134.67	G 51.14		
Co ₉ S ₈	K_V 169.78	G_V 70.64	185.96	0.32
	K_R 169.78	G_R 70.51		
	K 169.78	G 70.58		

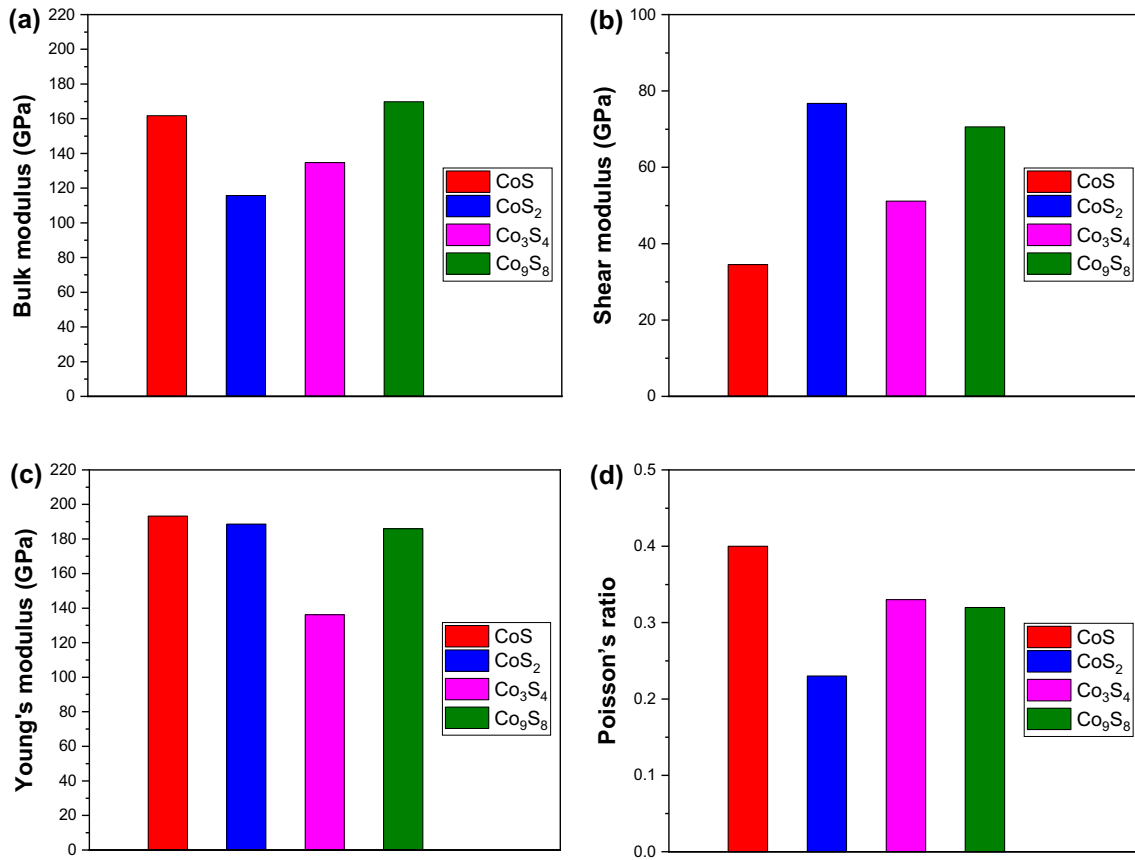


Figure 2. Bulk modulus, shear modulus, Young's modulus and Poisson's ratios of the four types of cobalt sulphides. (a) Bulk modulus; (b) shear modulus; (c) Young's modulus; (d) Poisson's ratio.

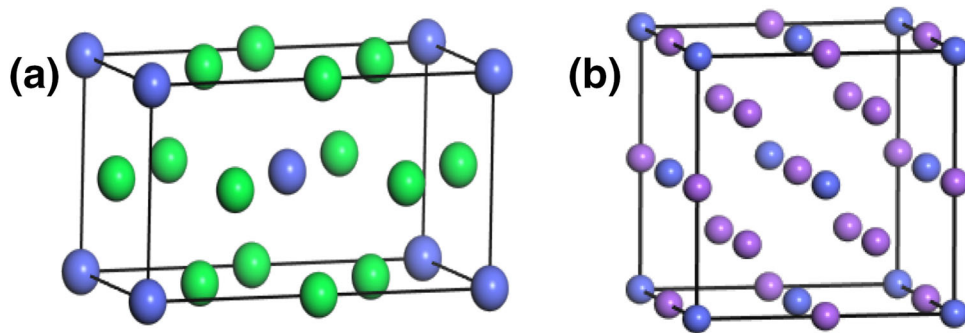


Figure 3. Crystal models of Li₃Co and Na₃Co phases. (a) Tetragonal Li₃Co and (b) cubic Na₃Co.

structure. The lattice parameters of the Li₃Co structure obtained from the theoretical calculation is consistent with the results previously reported [11]. The Na₃Co phase shows a cubic crystal structure as shown in figure 3b.

The elastic constants of Li₃Co and Na₃Co are shown in table 4, which can be employed to calculate the bulk modulus, shear modulus and Poisson's ratio of cobalt sulphides. For the tetragonal phase, the compliance constants S_{ij} can be expressed as follows [22].

$$\begin{aligned}
 S_{11} &= (C_{11}C_{33} - C_{13}^2)/[C(C_{11} - C_{12})] \\
 S_{12} &= (-C_{12}C_{33} + C_{13}^2)/[C(C_{11} - C_{12})] \\
 S_{13} &= -C_{13}/C \\
 S_{33} &= (C_{11} + C_{12})/C \\
 C &= C_{33}(C_{11} + C_{12}) - 2C_{13}^2 \\
 S_{44} &= 1/C_{44} \\
 S_{66} &= 1/C_{66}
 \end{aligned}
 \tag{6}$$

Table 4. Calculated elastic constants C_{ij} of Li_3Co and Na_3Co .

Elastic constants C_{ij} (GPa)	Co_9S_8	Li_3Co	Na_3Co
C_{11}	268.93250	63.70038	17.25721
C_{22}	268.93250	63.70038	17.25721
C_{33}	268.93250	63.70038	17.25721
C_{12}	120.20748	24.23095	12.22648
C_{13}	120.20748	16.59411	12.22648
C_{23}	120.20748	16.59411	12.22648
C_{44}	68.15707	10.49726	15.63545
C_{55}	68.15707	10.49726	15.63545
C_{66}	68.15707	10.49726	15.63545

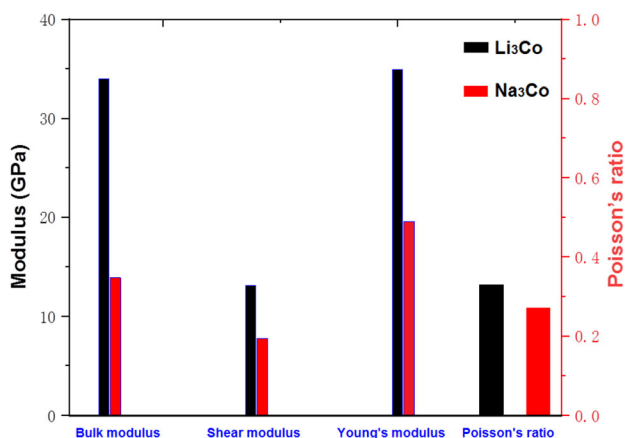


Figure 4. Bulk moduli, shear moduli and Poisson's ratios of Li_3Co and Na_3Co phases.

Then,

$$K_V = [2(C_{11} + C_{12}) + 4C_{13} + C_{33}]/9$$

$$K_R = 1/(2S_{11} + 2S_{12} + 4S_{13} + S_{33})$$

$$G_V = \frac{1}{15}(2C_{11} - C_{12} - 4C_{13} + C_{33} + 6C_{44} + 3C_{66})$$

$$G_R = \frac{15}{8S_{11} - 2S_{12} - 8S_{13} + 4S_{33} + 6S_{44} + 3S_{66}} \quad (7)$$

The obtained bulk moduli, shear moduli and Poisson's ratios of Li_3Co and Na_3Co are shown in figure 4. Generally, the Li_3Co and Na_3Co phases show much lower bulk modulus, shear modulus and Young's modulus than in the case of Co_9S_8 phase. It indicates that the lithium/sodiation induces the degradation of the mechanical properties of Co_9S_8 phase. The low bulk modulus means that the Li_3Co and Na_3Co phases cannot resist the repeated Li insertion/extraction during the cycling process. The low mechanical stability of Li_3Co and Na_3Co phases further causes the cracking and pulverization in the electrodes. This is the reason why the raw Co_9S_8 phase exhibits poor cycling performance. The values of bulk modulus and shear modulus of Li_3Co are higher than that of Na_3Co . The experimental results indicated that Co_9S_8 material delivered

higher discharge capacity and better cycling performance in the Li-storage than in the case of Na-storage. From this viewpoint, carbon coating technology can improve the electrochemical properties of Co_9S_8 by enhancing its mechanical stability.

4. Conclusion

In summary, the bulk moduli, shear moduli, Young's moduli and Poisson's ratios of the four types of cobalt sulphides have been calculated. Among them, the Co_9S_8 phase exhibits a relatively high bulk modulus of 169.78 GPa, showing great potential as anode materials for Li and Na storage. After lithiation/sodiation process, Li-Co alloys including Li_3Co and Na_3Co phases have been formed. The mechanical properties of the Li_3Co and Na_3Co phases have also been calculated. The low bulk modulus indicates that the Li_3Co and Na_3Co phases cannot resist the repeated Li insertion/extraction during the cycling process. As comparison, the Li_3Co phase shows better mechanical properties than the Na_3Co phase.

Acknowledgements

This work was financially supported by the Key Laboratory of Intelligent Computing and Information Processing of Ministry of Education and High-level Talent Gathering Project in Hunan Province (No. 2019RS1059).

References

- [1] Chen H, Zhang W, Tang X-Q, Ding Y-H, Yin J-R, Jiang Y *et al* 2018 *Appl. Surf. Sci.* **427** 198
- [2] Chibueze T C and Okoye C M I 2019 *Physica B* **554** 165
- [3] Ding Y, Jiang Y, Xu F, Yin J, Ren H, Zhuo Q *et al* 2010 *Electrochem. Commun.* **12** 10
- [4] Fuchsichler B, Stangl C, Kren H, Uhlig F and Koller S 2011 *J. Power Sources* **196** 2889
- [5] Hassoun J, Bonaccorso F, Agostini M, Angelucci M, Betti M G, Cingolani R *et al* 2014 *Nano Lett.* **14** 4901
- [6] Jiang T, Yang S, Dai P, Yu X, Bai Z, Wu M *et al* 2018 *Electrochim. Acta* **261** 143
- [7] Jiang W, Han Y, Jiang Y, Xu F, Ouyang D, Sun J *et al* 2021 *Appl. Clay Sci.* **203** 106020
- [8] Jiang W, Jiang Y, Zhao S, Peng J, Qin W, Ouyang D *et al* 2020 *Energy Technol.* **8** 1901262
- [9] Jiang W, Liu Q, Peng J, Jiang Y, Ding Y and Wei Q 2020 *Nanotechnol.* **31** 235713
- [10] Liu X, Jiang Y, Li K, Xu F, Zhang P and Ding Y 2019 *Mater. Res. Bull.* **109** 41
- [11] Liu Y, Sun K, Jiang J, Zhou W, Shang Y, Du C *et al* 2021 *Green. Energy Environ.* **6** 91
- [12] Qu G, Wu T, Yu Y, Wang Z, Zhou Y, Tang Z *et al* 2019 *Nano Res.* **12** 2960

- [13] Shadike Z, Cao M-H, Ding F, Sang L and Fu Z-W 2015 *Chem. Commun.* **51** 10486
- [14] Sun J, Lu C, Tian Q, Mei Y, Peng J and Ding Y 2020 *Appl. Surf. Sci.* **513** 145756
- [15] Tan J, Li Y and Ji G 2012 *Comput. Mater. Sci.* **58** 243
- [16] Wang Z, Li F, Ding W, Tang X, Xu F and Ding Y 2021 *Nanotechnol.* **32** 315707
- [17] Xiao C, Tang X, Peng J and Ding Y 2021 *Appl. Surf. Sci.* **563** 150278
- [18] Xiao Q, Fan Y, Wang X, Susantyoko R A and Zhang Q 2014 *Energy Environ. Sci.* **7** 655
- [19] Xu X, Liu W, Kim Y and Cho J 2014 *Nano Today* **9** 604
- [20] Yang Z, Ding Y, Jiang Y, Zhang P and Jin H 2018 *Nanotechnol.* **29** 405602
- [21] Zhang R, Lu C, Shi Z, Liu T, Zhai T and Zhou W 2019 *Electrochim. Acta* **311** 83
- [22] Zhang W, Yin J, Zhang P, Tang X and Ding Y 2018 *J. Mater. Chem. A* **6** 12029
- [23] Hill R 1952 *Proc. Phys. Soc.* **65** 349
- [24] Apostolova R, Shembel' E, Talyosef I, Grinblat J, Markovsky B and Aurbach D 2009 *Russ. J. Electrochem.* **45** 311